ChemComm

ROYAL SOCIETY OF CHEMISTRY

FEATURE ARTICLE

View Article Online
View Journal

Cite this: DOI: 10.1039/d4cc01889c

Extrusion-based 3D printing of soft active materials

Jiayu Zhao,[a] Xiao Li,[b] Donghwan Ji[a] and Jinhye Bae *[ab]

Received 22nd April 2024,
Accepted 11th June 2024

DOI: 10.1039/d4cc01889c

rsc.li/chemcomm

Active materials are capable of responding to external stimuli, as observed in both natural and synthetic systems, from sensitive plants to temperature-responsive hydrogels. Extrusion-based 3D printing of soft active materials facilitates the fabrication of intricate geometries with spatially programmed compositions and architectures at various scales, further enhancing the functionality of materials. This Feature Article summarizes recent advances in extrusion-based 3D printing of active materials in both non-living (*i.e.*, synthetic) and living systems. It highlights emerging ink formulations and architectural designs that enable programmable properties, with a focus on complex shape morphing and controllable light-emitting patterns. The article also spotlights strategies for engineering living materials that can produce genetically encoded material responses and react to a variety of environmental stimuli. Lastly, it discusses the challenges and prospects for advancements in both synthetic and living composite materials from the perspectives of chemistry, modeling, and integration.

Introduction

Active materials, characterized by their responsiveness to environmental stimuli, such as temperature,[1] light,[2] electric,[3] and magnetic fields,[4] are revolutionizing various technological domains. These materials can actively change their properties, including shape,[5] optical properties,[6] mechanical,[7] chemical,[8] and so on,[9] in response to external conditions. This adaptability makes them pivotal in advancing smart technologies and sustainable solutions.

The concept of "active materials" evolved from the "active matters" that was rooted in biology, specifically in the study of systems exhibiting self-propelled motion, such as flocks of birds or schools of fish.[10] Subsequently, physicists have become increasingly interested in such phenomena. They are particularly focused on forms of movement, growth, self-assembly, and self-organization that can be quantified and explained using the principles of physics,[11] which further expand the concept of "active matters" in both living and non-living systems.

[a] Aiiso Yufeng Li Family Department of Chemical and Nano Engineering, University of California San Diego, La Jolla, CA 92093, USA. E-mail: j3bae@ucsd.edu
[b] Material Science and Engineering Program, University of California San Diego, La Jolla, CA 92093, USA

Jiayu Zhao

Jiayu obtained her PhD degree in the NanoEngineering Department at the University of California San Diego. She received her BS in Polymer Science and Engineering at Beijing University of Chemical Technology in 2017, and her MS in Macromolecular Science and Engineering at Case Western Reserve University in 2019. Her research interests are stimuli-responsive soft materials with programmable behaviors.

Xiao Li

Xiao Li is a PhD student in the Materials Science and Engineering program under the supervision of Prof. Jinhye Bae. His research interests lie in the stimuli-responsive hydrogels and 3D printing of smart polymers. He received his bachelor's degree at Nanjing Tech University in China. In 2019, he obtained his master's degree at the University of Chinese Academy of Sciences. In 2021, he joined Prof. Bae's lab and started working as a graduate student researcher at the University of California San Diego.

This phase focused on understanding how the movement of individual components contributes to collective behavior in non-equilibrium systems. In the first twenty-first century, the definition broadened to encompass materials responding to external stimuli in more subtle ways. It began to include materials that change their physical states (*e.g.*, shape-memory alloys, *etc.*), or chemical compositions, as observed in responsive polymers, inspired by biological systems. In this Featured Article, we define ''active materials'' as the materials that can respond to certain conditions and actively change their state to fulfill a specific function due to the design of the materials' structure and composition, which slightly refined the definition of ''active materials'' from Fratzl *et al.*[12]

Traditionally, active materials have been fabricated using various methods including mold casting,[13] electrospinning,[14] and photolithography.[15] However, these methods offer limited design space in terms of structural intricacy. 3D printing, also referred to as additive manufacturing, overcomes these limitations by facilitating the creation of active materials in any desired shape with high precision.[16] This process allows for integrating the responsiveness of materials into their structural designs, unlocking new functional capabilities. Ji *et al.* utilized digital light processing (DLP) 3D printing and Fe_3O_4 incorporated photo-crosslinkable resins to fabricate magnetic responsive structures with arbitrary shapes.[17] By printing the magnetic and nonmagnetic segments alternatively, multiple magnetically driving devices or actuators, like the cargo-catching gripper, were achieved readily. Similarly, Zarek *et al.* combined shape memory polymers (SMPs) with stereolithography (SLA) 3D printing to generate high-resolution 3D shape memory structures.[18] The shape memory property of printed SMPs enabled fast shape change upon heating the environmental temperature, laying the foundation for obtaining temperature sensors and electrically driving actuators *via* combining the Joule heating of conductive layers. In addition to these 3D printing technologies, extrusion-based 3D printing, a 3D printing technique that involves the extrusion of a viscoelastic ink through a nozzle to create structures layer by layer,[19] has become a popular method to fabricate active materials due to its ability to precisely control the deposition of materials with complex rheological properties.[20] Such ability is crucial for active materials, which often requires specific structural or compositional arrangements to respond effectively to environmental stimuli. In addition, extrusion-based 3D printing is utilized for manufacturing a wide range of stimuli-responsive materials, including shape-memory polymers,[21] liquid crystal elastomers,[22] hydrogels,[20] and cell-laden biomaterials.[23] New functionalities can be unlocked by incorporating these stimuli-responsive properties into customized structural designs. Furthermore, extrusion-based 3D printing allows for the integration of multiple materials with varied functionalities and properties in a single print,[24] enabling the creation of structures with intricate geometries and internal architectures in microscale.[25] The macroscale architecture is pre-designed using 3D Computer-Aided Design (CAD) software for the target application, while the microscale architecture is governed by material compositions, shear stress generated in the printing nozzle, and the post-curing process if applicable (Fig. 1). For instance, biomimetic shape morphing was achieved through the anisotropic swelling of the hydrogel matrix, driven by the shear stress-induced alignment of cellulose.[26] Sequential self-folding was realized by varying the swelling kinetics of the nanocomposite hydrogel, with phase-separated micro-domains induced by the post-curing process.[27] Additionally, more complex microscale architectures can be developed by utilizing orthogonally induced differentiation of stem cells, enabling the creation of bio-printed organoids with a pervasive vascular network.[28] Micro-architecture also plays a crucial role in determining the rheological properties of inks, facilitating extrusion-based 3D printing of previously unprintable materials. For example, mechanoluminescence devices can be printed into complex geometries that were

Donghwan Ji

Donghwan Ji is a Postdoctoral Scholar at the University of California San Diego. He received his PhD degree in Chemical Engineering from Sungkyunkwan University (SKKU) in 2022. His research focuses on topics in materials science and engineering and chemical engineering for developing mechanically reinforced composite materials (bioplastics and hydrogels), hydrogel-based bioelectronics, stimuli-responsive hydrogels, quasi-solid gel electrodes and electrolytes, and their 3D printing techniques.

Jinhye Bae

Jinhye Bae is an Assistant Professor in the Department of Nano-Engineering at the University of California San Diego. She received her PhD in Polymer Science and Engineering at the University of Massachusetts Amherst in 2015, and then worked as a Postdoctoral Fellow in the School of Engineering and Applied Sciences at Harvard University. Her research focuses on understanding the physical and chemical properties of polymeric materials to program their shape reconfiguration and responsiveness. Her research interests also include the integration of material characteristics into new structural design and fabrication approaches for applications in biomedical devices, soft robotics, actuators, and sensors.

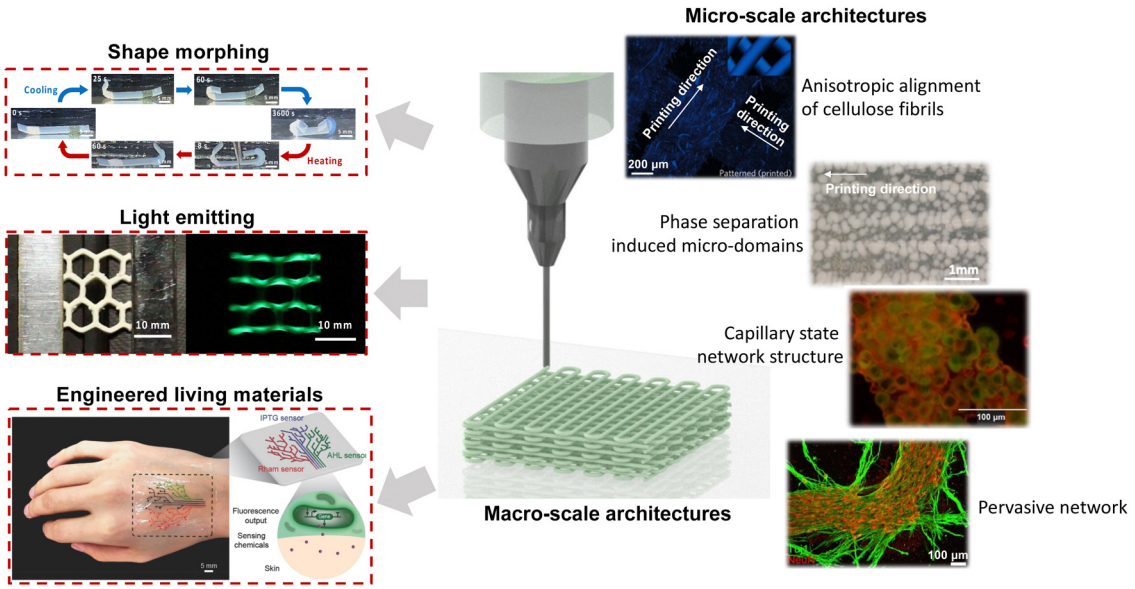

Fig. 1 Representations of extrusion-based 3D printing of active materials, featuring tailored architectures, ranging from the macro to the micro scale, for the fabrication of shape-morphing, light-emitting, and engineered living materials systems. Reprinted with permission from ref. 26–29,32 Copyright 2022 and 2016 Springer Nature, 2018 and 2022 John Wiley, and 2022 Elsevier.

previously unattainable by leveraging the capillary state of granular systems.[29] These capabilities are essential for the development of advanced active materials used in applications such as soft robotics,[30] smart sensors,[31,32] and biomedical devices,[28,33] where precision and material complexity are key.

To achieve complex structures with high resolution (for example, below 1 mm), the ink used in extrusion-based 3D printing typically has tailored rheology, ensuring it is fluid enough to flow through the nozzle but solidifies quickly upon deposition.[34] To meet these requirements, inks with shear-thinning properties are required, as they exhibit reduced viscosity under increased shear rate, facilitating pressure-regulated flows.[35] These inks should also possess sufficient yield strength to support the structure of the 3D-printed material and the weight of subsequent layers. While solutions, colloids, hydrogels, emulsions, and pastes are commonly used, they often display low viscosity and stiffness, necessitating reformulation for desired rheological properties (viscosity ranging from 10^2 to 10^6 mPa s at a shear rate of 0.1 s^{-1}).[35] Adjusting temperature, pH, and ionic strength, along with incorporating hardening agents or nano fillers, can enhance the rheological properties. Such rheological modifications, aimed at optimizing flow and curing, are compatible with a variety of stimuli-responsive materials as previously mentioned.

In this Feature Article, we aim to give a brief overview of the new functionality of active materials enabled by their micro- and macroscope structure design through ink formulation and extrusion-based 3D printing, respectively, based on our work and related studies by peers (Fig. 1). This Feature Article is structured into two main sections. Firstly, we discuss the progress in extrusion-based 3D printing of synthetic active materials for non-living systems (*i.e.*, synthetic systems), highlighting how material features are integrated into novel structural designs. In this section, we will mainly cover two topics based on their functionality—shape morphing and light-emitting. Secondly, we explore recent advancements in fabricating bioactive scaffolds, cell-laden structures, and plant-synthetic polymeric hybrids using extrusion-based 3D printing for living systems. Finally, we will address the existed limitations and envisage future developments in the next generation of active materials fabricated by extrusion-based 3D printing.

Extrusion-based 3D printing of active materials in the non-living system

Shape morphing of active materials

Shape change in response to environmental cues is ubiquitous in plants through various strategies including cellular organization, anisotropic cellulose fiber orientation, and mechanical instabilities.[36] The strategies for shape changes found in plants have greatly inspired researchers in designing shape morphing actuators using synthetic active materials,[37] particularly in terms of the local material composition and internal structure. One of the key considerations for realizing programmable shape morphing of synthetic materials is the introduction of anisotropy into the material system by varying the crosslinking density, material distribution, or filler orientation. (Table 1) Gladman *et al.* demonstrated a reversible and complex shape change of the hydrogel composite by incorporating the stiff and high-aspect-ratio cellulose fibrils in the soft hydrogel ink *via* extrusion-based 3D printing.[26] The shear force-induced alignment of the cellulose fibrils during the printing process endows anisotropic swelling and mechanical properties in each layer. By patterning the anisotropically-filled hydrogel ink into the pre-determined pattern driven by the theoretical model,

Table 1 Summary of materials, stimuli and mechanisms employed in shape morphing of synthetic active materials using extrusion-based 3D printing

Materials	Stimuli	Shape morphing mechanism	Ref.
PNIPAM + NFC + nanoclay	Hygroscopic	Shear force-induced alignment of cellulose created anisotropic swelling of PNIPAM	26
Polyurethane + carbon black	Light	Shape recovery of polyurethane triggered by photothermal effect	38
Silicone + NdFeB alloy + fumed silica nanoparticles	Magnetic	Magnetic polarity created by magnetic field aligned ferromagnetic particles during printing	39
Co-polyester + fibrous filler + ABS	Hygroscopic	Combination of anisotropy created by oriented fibrous and integration of ABS	40
PDMS + glass fibers/PNIPAM + NFC	Chemical and hygroscopic	Anisotropic materials combined with bistable structures	41
Epoxy	Heat	Anisotropy introduced by different crosslinking density of epoxy	42
PDMS + fumed silica nanoparticles + PNIPAM + nanoclay	Hygroscopic and heat	Combination of anisotropy created by the integration of dissimilar materials and phase-separation induced micro-domains	27

PNIPAM = poly(*N*-isopropylacrylamide); NFC = nanofibrillated cellulose; NdFeB = neodymium–iron–boron; PDMS = polydimethylsiloxane; ABS = acrylonitrile Butadiene Styrene.

programmable shape morphing can be achieved upon immersing in water. (Fig. 2(a)) Drawing inspiration from sunflowers, Yang *et al.* created a photo-responsive shape memory model, combining polyurethane and photo-responsive carbon black.[38] Similarly, Kim *et al.* introduced anisotropic alignment of ferromagnetic microparticles by applying a magnetic field to the dispensing nozzle during printing,[39] enabling a fast-transitioning, magnetically responsive soft material with complex shape transformations. (Fig. 2(b)) Meanwhile, Correa *et al.* developed a bilayer region mimicking the motion of pine cone scales,[40] (Fig. 2(c)) and Jiang *et al.* printed bistable structures for rapid actuation, akin to a Venus flytrap.[41] Additionally, Wang *et al.* engineered an artificial *M. pudica* actuator, demonstrating plant-like movements.[42]

Although complex shape morphing has been achieved in the examples mentioned above, some applications require sequential shape morphing to perform specific tasks. In general, there are three strategies widely applied to create sequential folding: (1) altering the external stimulus chronologically;[43] (2) varying chemical compositions of active materials allowing them

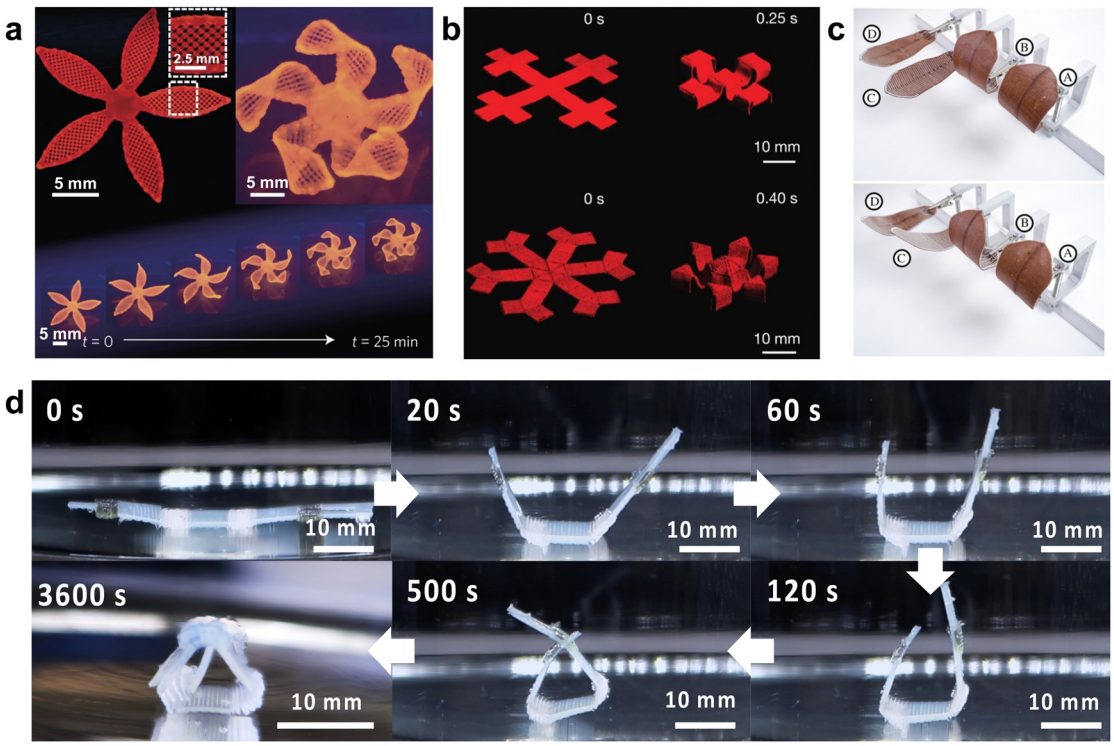

Fig. 2 (a) Bilayers with programmed orientations determined by the printing path, with time-lapse sequences of the flowers during the swelling process. Reprinted with permission from ref. 26 Copyright 2016 Springer Nature. (b) Photographs of quadrupedal (top) and hexapedal (bottom) structures enabled by folding of the magnetically active segments surrounding the magnetically inactive segments. Reprinted with permission from ref. 39 Copyright 2018 Springer Nature. (c) Printed scales show different shape deformations when fully wet. Reprinted with permission from ref. 40 Copyright 2022 The Royal Society of Chemistry. (d) Photographs of the self-locking latch structure during swelling at 22 °C. Reprinted with permission from ref. 27 Copyright 2022 John Wiley.

to exhibit different folding speeds under the same stimulus;[44] and (3) altering the dimensions of the active materials.[45] However, sequential folding using a single active material, without changing chemical composition or design under a static stimulus is highly desired, as it can greatly simplify the fabrication process while improving structural integrity with a more generalized actuation process. Our group has recently addressed this gap by utilizing a 3D-printed hinge-based bilayer structure composed of a polydimethylsiloxane (PDMS) layer as the passive matrix and a temperature-responsive nanocomposite hydrogel as the active hinge.[27] The nanocomposite hydrogel comprises poly(*N*-isopropylacrylamide) (PNIPAM) for temperature responsiveness and nanoclay (NC) as a rheological modifier to enable extrusion-based 3D printing. The strain mismatch generated between the un-swellable PDMS layer and the swellable NC-PNIPAM hydrogel upon immersing in water below lower critical solution temperature (LCST, $\sim$22 °C) induces folding. Further increasing the temperature above LCST causes the folded structure to flatten due to the de-swelling of the NC-PNIPAM. The characteristic feature of the NC-PNIPAM is that adjusting the intensity of ultraviolet (UV) light during its photo-crosslinking process enables the creation of distinguished microstructures through phase separation mechanisms, facilitating control over the folding speed. At low UV intensity ($\approx$10 mW cm^{-2}), spinodal decomposition was observed between the NC and PNIPAM matrix, whereas higher UV intensity ($\approx$100 mW cm^{-2}) produced a transparent matrix with a relatively homogeneous microstructure. The unique heterogeneous microstructure presented in the microphase-separated NC-PNIPAM creates swelling gradient in the matrix, dramatically decreasing the characteristic time of swelling by one order of magnitude compared to the one with a homogenous microstructure. By integrating these two types of NC-PNIPAM within one structure *via* extrusion-based 3D printing, a self-locking latch structure (Fig. 2(d)) was demonstrated to highlight the reversible sequential self-folding ability. The nanocomposite hydrogel-PDMS bilayer system has been successfully realized with precise responsiveness, enabling control over both its final shape and folding speed. This was achieved through extrusion-based 3D printing and subsequent processes (*i.e.*, UV curing intensity), which enable the system to carry out specific tasks (*i.e.*, self-locking) autonomously. This study underscores the critical influence of material structure at various scales, from micro to macro, in defining physical properties and, consequently, their potential applications.

Extrusion-based 3D printing of mechanoluminescence devices

As technology demands evolve rapidly, traditional rigid light-emitting devices such as liquid crystal displays prove inadequate due to their lack of flexibility, making them unsuitable for emerging wearable device applications. The quest for flexibility and durability has turned the spotlight on mechanoluminescence (ML),[46] a self-powered light emission process activated by external mechanical stimuli such as rubbing, bending, stretching, or compression. This phenomenon, first recorded by Francis Bacon in 1605 when he noticed light emission upon scraping sugar with a knife,[47] has since been observed in a variety of hard materials including quartz, rocks, aluminates, and alkali halides. However, such ML materials typically cannot withstand repeated activation as they often incur permanent damage (*i.e.*, fracture) post-emission. The most prevalent ML materials in use today are those that are durable and capable of maintaining a high brightness level *(i.e.*, hundreds of candelas per square meter) after thousands of cycles.[48]

Integrating these kinds of durable ML materials into soft devices brings forth a revolution, especially in precision healthcare,[49] personal electronics,[50] and artificial skin.[48] Their ability to conform to irregular shapes with high durability enables applications including advanced wearables, dynamic displays, and healthcare monitoring devices, where strong and repeatable luminescence is required. The resilience of soft ML materials, which can emit light under mechanical stress without breaking, positions them as prime candidates for next-generation technologies, expanding their scope beyond the limitations of their hard counterparts and promising exciting advances in areas like visual feedback, improved visibility in low-light conditions, and *in vivo* applications.

Traditional ML devices are composed of ML materials with polymer matrices such as PDMS or epoxy resin fabricated *via* mold casting or coating,[51,52] which inherently limits its functionality due to the lack of geometry complexity and mechanical tunability. On the other hand, extrusion-based 3D printing offers a solution to create ML devices with specially controlled composition and geometries. (Table 2) The primary challenge in using extrusion-based 3D printing to fabricate ML devices lies in developing an appropriate ML ink with optimal rheological properties including shear-thinning, solid-like behavior, and sufficient yield stress. Qian *et al.* developed a printable ML ink that comprised of ZnS:Mn^{2+}/Cu^{2+}@Al_2O_3 microparticles, PDMS, and SiO_2 nanoparticles (NPs) (Fig. 3(a)), in which the SiO_2 not only served as the rheological modifiers but also focus

Table 2 Summary of recent progress in extrusion-based 3D printing of ML devices

Materials	Printing strategy	Geometry	Target applications	Ref.
PDMS + ZnS:M^{2+}(Mn/Cu)@Al_2O_3 + fumed silica nanoparticles	High loading of fumed silica nanoparticles	2D planar	Photonic skin	53
PDMS + ZnS doped with transition metal ions	Temperature modulation	2D planar and 3D ring	Embedded sensors and energy devices	54
PDMS + ZnS:Cu + fumed silica nanoparticles	Capillary state of granular system	2D and 3D cellular structures	Wearable sensors	29

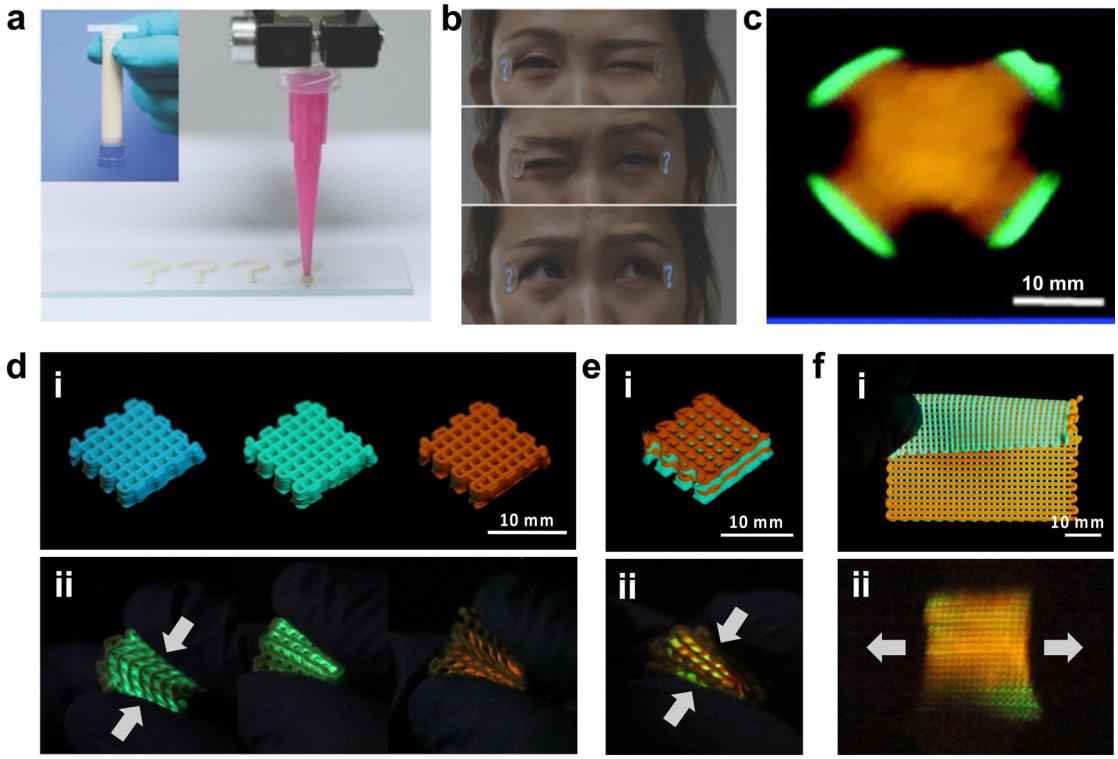

Fig. 3 (a) Extrusion-based 3D printing of the ML ink consisting of pre-cured microbeads of ZnS:Cu/PDMS, a secondary PDMS precursor and SiNPs; (b) The skin-driven various color ML response to canthus muscle movements. Reprinted with permission from ref. 53 Copyright 2018 John Wiley. (c) Photograph of the printed dual color ML planar sheet, with light emission by diagonal compression and release. Reprinted with permission from ref. 54 Copyright 2018 The Royal Society of Chemistry. (d) Photographs of the printed ML 3D lattice structures ($10 \times 10 \times 4\ mm^3$) with different colors (*i.e.*, blue, green, and orange, respectively) emitted under (i) UV irradiation and (ii) manual compression, respectively. (e) Photographs of the printed dual-color (*i.e.*, green and orange) ML 3D lattice structure ($10 \times 10 \times 4\ mm^3$) with interlayer design under (i) UV irradiation and (ii) manual compression, respectively. (f) Photographs of the printed 2D lattice sheet ($50 \times 50 \times 1.2\ mm^3$) with ink containing orange ML phosphor on the top and green phosphor on the bottom under (i) UV irradiation (half of the sample is flipped to better visualize the green color at the bottom) and (ii) manual stretching, respectively. Reprinted with permission from ref. 29 Copyright 2022 Elsevier.

stress onto the ML microparticles, enabling intense ML under weak stress stimuli by skin movement.[53] (Fig. 3(b)) Another work demonstrated by Patel *et al.* used extrusion-based 3D printing to integrate ML materials with different colors,[54] which can produce anisotropic light emission upon compression from different directions. (Fig. 3(c)) The printed structures shown in these studies, while innovative, remain fundamentally basic in terms of the geometry design and could similarly be produced using conventional mold casting techniques. Our team has recently created an ink formulation that enables extrusion-based 3D printing of periodic cellular structures with high resolution, approximately 400 micrometers. This was achieved by meticulously tuning the rheological properties of the ink to harness capillary forces within the ink, which consists of pre-cured microbeads of ZnS:Cu/PDMS, a secondary PDMS precursor and silicon nanoparticles (SiNPs).[29] Initially, the microbeads were created by curing a mix of ZnS:Cu/PDMS in water at 80 °C for 90 minutes with vigorous stirring, resulting in cross-linked microbeads. The secondary PDMS precursor, which shares a chemical affinity with the microbeads, was then introduced to act as a wetting agent, ensuring the surfaces of microbeads were adequately coated and thus formed a capillary state.[55,56] Subsequently, silica nanoparticles (SiNPs) were incorporated to not only improve the printability of the ink but also to amplify the luminance intensity of the final ML device by efficiently transferring the stress to deform the PDMS when subjected to an external load. The enhancement of viscosity is attributed to the network of connections formed between SiNPs. The combined effect of the secondary PDMS precursor and SiNPs successfully transformed the initial liquid suspension into a paste-like capillary ink. The rheology optimization strategy can be applied to different kinds of ZnS:Cu phosphors that allow different color emissions (Fig. 3(d)). By utilizing the dual printing technique, inks with different colors can be integrated into one single lattice structure (Fig. 3(e)-i),[29] showcasing the concurrent emission of both colors under manual compression (Fig. 3(e)-ii). Furthermore, a flexible 2D lattice sheet was printed, exemplifying a battery-free, dual-color textile with green and orange hues printed orthogonally to one another (Fig. 3(f)-i). When subjected to unidirectional stretching, this lattice sheet emits both colors in a pre-defined pattern that corresponds to the orientation of the printing. (Fig. 3(f)-ii) With the ability to fabricate ML materials into complex geometry, we also discovered anisotropic and isotropic luminescence using

structures with positive and negative poisson ratios, respectively. The versatile structure design also endows the ML materials with tunable mechanical properties with Young's modulus ranging from 3.5 to 19 kPa.[29] The programmable light-emitting patterns and adjustable mechanical characteristics of the 3D-printed ML material open new avenues for self-powered optical wearable stress sensors and interactive electronic skins.

Engineered living materials with stimuli-responsiveness

The rapid development of synthetic active materials is inspired by living materials that exhibit stimuli-responsive properties.[57,58] In recent years, the emerging field of engineered living materials (ELMs) that integrate synthetic materials with living materials has attracted lots of interest,[59,60] because it can create composite materials that are responsive to diverse stimuli and capable of generating complex, genetically encoded material outputs. Such ELMs patterned by extrusion-based 3D printing have precise control over material properties and function, opening new avenues for applications including biosensing, chemical threat decontamination, soft robotics, and drug delivery. Recent progress in ELMs is summarized in Table 3 and discussed in the following paragraph. Generally, the ELMs contain living organisms with responsive functions and polymeric matrices serving as a scaffolding function.[60] The polymeric matrices should be biocompatible materials that serve as an extracellular matrix to provide a congenial environment for the growth of living cells, ensuring they do not negatively impact essential functions such as nutrient transport, gas exchange, and photosynthesis. Additionally, these matrices must be resistant to biodegradation caused by living organisms to maintain their structural integrity and functionality. Genetic engineering of these cells enables complex responses to environmental stimuli. Duraj-Thatte *et al.* designed a microbial ink for 3D printing (Fig. 4(a)), and demonstrated the printed structure for therapeutic application (Fig. 4(b)-i), sequestration of a toxic chemical (Fig. 4(b)-ii), and regulation of cell growth (Fig. 4(b)-iii).[61] They have fully leveraged microbial engineering to develop the bioink with high cell viability/compatibility and proper rheological properties that are a good extrudability of the printing ink and shape integrity of the printed structure. CsgA-α and CsgA-γ were expressed from specifically engineered *Escherichia coli* (*E. coli*) strain (PQN4), resulting in the formation of nanofibers with supramolecular crosslinking (*i.e.*, the culture of engineered nanofibers) (Fig. 4(a)). These microbial cultures were filtrated, and a viscoelastic printable hydrogel as microbial ink was obtained. On purpose, *E. coli* cells were additionally modified/programmed and introduced to fabricate functional microbial ink (Fig. 4(b)). As a first example, they employed isopropyl β-D-1-thiogalactopyranoside (IPTG), which is a chemical inducer, to signal the *E. coli* (PQN4-Azu) and consequently to synthesize an anticancer biologic drug (azurin) (Fig. 4(b)-i). The printed structure with the PQN4-Azu secreting azurin played a role as a therapeutic living architecture. They also fabricated a microbial ink that can sequester a toxic chemical, for example, Bisphenol A (BPA) (Fig. 4(b)-ii). A BPA-binding peptide domain was grafted to the CsgA (CsgA-BPABP), and *E. coli* cells expressing CsgA-BPABP (PQN4-BPA) were employed in the microbial ink for the sequestration living material. Furthermore, they modified *E. coli* cells to express endoribonuclease toxin, MazF (PQN4-MazF) (Fig. 4(b)-iii). The printed structure comprising the PQN4-MazF-based living material implemented a regulation system that reduces and restores cell growth.

Similarly, Datta *et al.* employed engineered cyanobacterium *Synechococcus elongatus* PCC 7942 (*S. elongatus*) to implement stimuli-responsiveness (*e.g.*, fluorescence and bioremediation) of printed structures (Fig. 4(c)–(e)).[62] The combination of alginate polymer and genetically engineered cyanobacterial cells produced a viscoelastic printable hydrogel as microbial ink (Fig. 4(c)). The influx and efflux of gas, nutrients, and metabolites through a printed hydrogel enabled the embedded cyanobacterial cells to grow or induce gene expression by

Table 3 Summary of recent progress in ELMs

Synthetic materials	Living organisms	Function of living organisms	Target applications	Ref.
Genetically engineered ECM of *E.coli* biofilm	Programmed *E.coli*	Facilitate the formation of 3D printable hydrogel ink and produce an anticancer drug in response to a chemical inducer	Therapeutical and biomedical applications	61
Alginate	Engineered cyanobacteria	Provide responsiveness through photosynthesis	Bioremediation	62
(PEDOT)-S:H	*Rosa floribunda*	Serve as vascular circuits	Sensors and electrochemical fuel cells	63–65
Engineered SWCNTs	Spinach	Transport the chemical cue from ground	Chemical monitors	66
Engineered nanoparticles including SNP-Luc, PLGA-LH_2, CS-CoA, and semiconductor nanocrystal phosphors	Spinach, arugula, watercress and kale	Independent energy source for enabling the chemical reaction of the nanoparticles	Self-powered photonics	67
PDMS + Au nanomesh + PAA hydrogel	Venus flytrap	Actuation subject	Plant-based actuators	68
PNIPAM + Nanoclay + graphene oxide	Spinach	Non-swellable substrate	Soft actuators	69

ECM = extracellular matrix; PEDOT = poly(3,4-ethylenedioxythiophene); SWCNTs = single-walled carbon nanotubes; SNP-Luc = firefly luciferase conjugated silica; PLGA-LH_2 = poly (lactic-*co*-glycolic acid); CS-CoA = coenzyme A functionalized chitosan; PAA = polyacrylic acid.

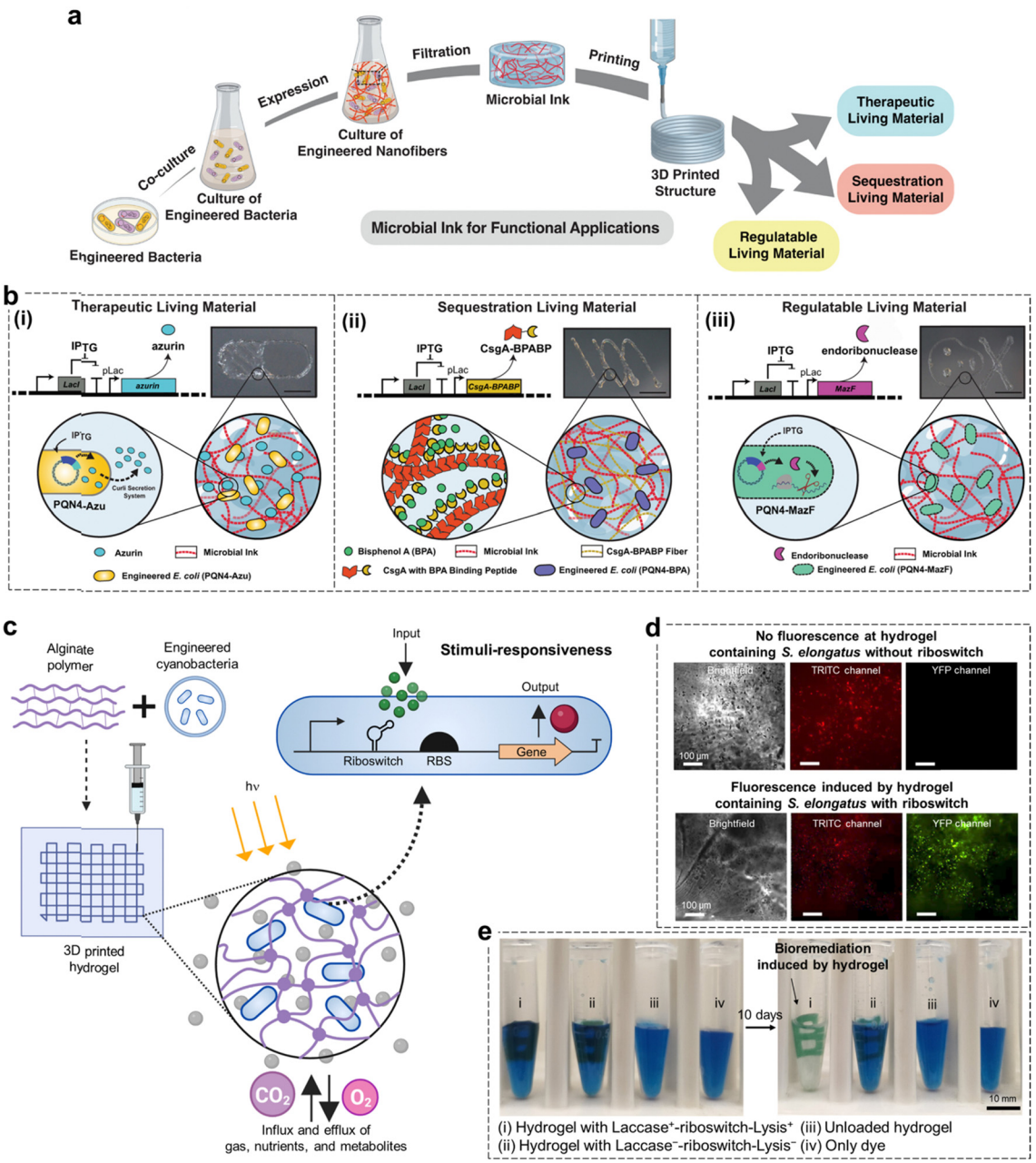

Fig. 4 Schematic illustration depicting the (a) fabrication of microbial ink and 3D printing of the ink; and (b) applications of the printed structure as (i) therapeutics synthesizing a drug (therapeutic living material), (ii) sequestration of a toxic chemical (sequestration living material), and (iii) regulation of cell growth (regulatable living material). Reprinted with permission from ref. 61 Copyright 2021 Springer Nature. (c) Schematic illustration depicting the fabrication and 3D printing of the ink and the mechanism of stimuli-responsiveness of the printed hydrogel by external cues. (d) Representative fluorescence microscopy images of each hydrogel containing *S. elongatus* strain with and without riboswitch, respectively. Images were taken under brightfield, TRITC channel, and YFP channel, respectively. (e) Photographs of different groups containing (i) hydrogel with Laccase^{+}-riboswitch-Lysis^{+}, (ii) hydrogel with Laccase^{-}-riboswitch-Lysis^{+}, (iii) unloaded hydrogel, and (iv) only dye solution, before/after 10 days incubation period. Reprinted with permission from ref. 62 Copyright 2023 Springer Nature.

external stimuli. To regulate the expression of yellow fluorescent protein (YFP) in the hydrogel (Fig. 4(d)), the *S. elongatus* was transformed with a plasmid pAM5057 to have riboswitch. Because this engineered *S. elongatus* strain responded to the chemical inducer (theophylline), bright fluorescence was observed at the printed hydrogel containing *S. elongatus* with riboswitch when exposed to 1 mM theophylline medium, whereas no fluorescence was detected at the hydrogel containing *S. elongatus* without being transformed with riboswitch. Furthermore, to create a hydrogel with a bioremediation function (Fig. 4(e)), engineered hydrogels were prepared using S. *elongatus* strains with chromosomally integrated plasmids

for Laccase expression and a lysis riboswitch. Comparative immersion tests in indigo-dyed BG-11 medium demonstrated the superior decolorization capability of the Laccase-expressing strain over both the non-expressing control and blank hydrogels, confirming the engineered strain's potential in bioremediation applications. Taken together, developing ELMs is a promising approach to exquisitely manipulate microbes embeddable in a soft matrix and to develop soft matters (*i.e.*, hydrogels) to possess unique responsiveness to external stimuli, particularly biological cues.

In addition to incorporating living cells with synthetic polymeric materials, there has been an emerging trend to augment the ability of living plants for sensing and shape morphing that can potentially redefine the way plants interact with their environment and humans. Electronic functionality has been integrated into the plants by immersing the cut stem into poly(3,4-ethylenedioxythiophene) (PEDOT)-S:H solution.[63] The plant's xylem, a key part of its vascular system, demonstrated significant electronic conductivity of around 0.1 S cm^{-1}, meaning that the xylem can conduct electric charges over long distances within the plant. Such electronic plants also managed to function as touch sensors, motion sensors, or motion-detecting antennae.[64,65] Strano group pioneered the plant nanobionics field by empowering the plant with specifically designed nanoparticles,[70] enabling them to serve as autonomous devices that can monitor groundwater contaminants and communicate with smartphones using infrared signals.[66] Such engineered living plants are equipped with two types of near-infrared fluorescent nanosensors: one, made of carbon nanotubes linked to Bombolitin II peptide, detects nitroaromatic compounds by changing its infrared emission; the other, a stable reference signal, is made of polyvinyl-alcohol coated carbon nanotubes. These nanosensors, embedded in the leaf mesophyll, detected the accumulation of contaminants absorbed from the roots, allowing real-time monitoring and estimation of the time contaminants spend in different plant parts. Furthermore, a light-emitting plant, which offers a sustainable lighting solution, was achieved through the plant nanobionic approach by infiltrating the functional nanoparticles inside plant leaves.[67] Such functional nanoparticles were synthesized from firefly luciferin, luciferase, and/or coenzyme A encapsulated in biocompatible poly(lactic-*co*-glycolic acid) (PLGA), silica, and chitosan, achieving prolonged and bright luminescence in plants like watercress. The integration of organic electronics and functional nanoparticles into plants opens possibilities for new technologies, such as devices for delivering substances to plants or sensors for monitoring plant physiology. Such engineered living plants can enhance conventional plant science and agricultural approaches, including molecular genetic techniques, which are restricted to a limited number of genetically tractable species.[71]

In addition to general living plants, sensitive plants, such as Mimosa pudica and Venus flytrap, are known to have shape changes in response to external stimuli including touch, heat, or light.[72,73] Their stimuli-responsive properties have driven researcher to study the underlying mechanisms and subsequently, how to converge their responsiveness for new applications. For example, Li *et al.* demonstrated the on-demand closure of Venus flytrap lobes by interfacing them with a conformal electrode,[68] which is composed of a soft and adhesive hydrogel layer as the plant-contacting layer and gold (Au) nanomesh on PDMS as the electronic transduction layer. Inspired by this, we began to explore whether we could endow ordinary plants, those not naturally responsive to environmental cues, with the ability to morph their shape. For instance, this capability could allow plants to adapt by changing their configurations to conserve or collect more water during drought conditions. To achieve this goal, we started by integrating the stimuli-responsive NC-PNIPAM with the plant tissues, such that programmable shape control was achievable through thermal cues or UV light.[69] The NC-PNIPAM precursors were printed onto the silane-treated decellularized leaf surface with predesigned shape and spatial control (Fig. 5(a)), enabling seamless contact between the NC-PNIPAM and the decellularized leave surfaces (Fig. 5(b)). Furthermore, the silane chemistry ensured the strong adhesion between the NC-PNIPAM and the decellularized leaf surface through the formation of covalent bonds (Fig. 5(c)). This strong adhesion achieved at the interface of the plant-synthetic polymer enabled the leaf to fold upon immersing this bilayer structure in a water bath at room temperature (*i.e.*, 22 °C), due to the strain-mismatch generated between the swellable NC-PNIPAM and non-swellable decellularized leaves. The process was reversible due to the reversible swelling and de-swelling properties of the NC-PNIPAM (Fig. 5(d)). Note that it was also possible to embed the stimuli of interest to the plant-polymer hybrid by tuning the chemical formulation of the NC-PNIPAM. As a proof of concept, we demonstrated that the introduction of graphene oxide (GO) to the NC-PNIPAM formulation enables remote light responsiveness owing to the photothermal effect of GO.[13]

Note that the decellularized leaf tissue utilized in our study does not constitute a "living plant." To achieve our initial objective of developing a strategy to bridge synthetic polymeric

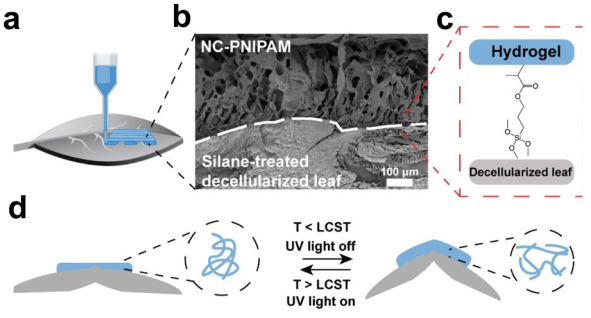

Fig. 5 (a) Schematic of depositing NC-PNIPAM precursor ink onto the decellularized leaf surface using extrusion-based 3D printing in perspective view. (b) Scanning Electron Microscope (SEM) images of the interface between NC-PNIPAM and silane-treated decellularized leaf. (c) Schematic of the adhesion mechanism. (d) Schematic of the reversible shape morphing in response to temperature and UV light change in side-view, with a folding angle of θ at equilibrium state. Reprinted with permission from ref. 69 Copyright 2022 American Chemical Society.

materials with living plants, we are currently working on creating biocompatible functional materials that can interface with living plants. This could open up new applications in agriculture and human–plant interactions. In essence, our work illuminates the concept of a 'plant cyborg,' allowing plants to perform functions beyond their native capabilities. The integration of synthetic polymers with plants could significantly advance agricultural development and may also lead to applications in plant-based soft actuators and robotics.

Conclusions and future prospects

The collective findings discussed in this paper underscore the significant strides being made in the realm of extrusion-based 3D printing of soft active materials in both non-living and living systems. The versatility of extrusion-based 3D printing allows for patterning active materials with tailored compositions and predesigned architectures, enabling more complex functionalities through rational structure design and multi-material integration. These 3D-printed functional materials pave the way for advanced applications across various interdisciplinary fields, including soft actuators/robotics, light-emitting devices, wearable sensors, biosensing, chemical threat decontamination, precise agriculture, *etc.* As we look towards the future, utilizing additive manufacturing, particularly extrusion-based 3D printing, for functional integration of active materials will undoubtedly play an important role in furthering material science research. The rapid advancement and expanding scope of these technologies, as evidenced in recent academic literature introduced in this Featured Article, strongly support this assertion, serving as a testament to their transformative potential in both scientific and technological landscapes. Despite the current progress, there are still many challenges and open questions remain:

The inverse design for active materials

Recent advancements in extrusion-based 3D printing technology have enabled the customized design of active materials, which plays a crucial role in the responsiveness and properties of materials. However, the structure design and ink formulation rely heavily on the empirical expertise of researchers and designers, based on their previous knowledge. This trial-and-error approach involving numerous structural possibilities significantly elevates the difficulty of selecting the optimal design and impedes the discovery of novel functionalities. Therefore, it would be highly beneficial to develop methods that can generate the appropriate structures directly correlated with the desired target properties, such as specific mechanical strengths, shape-morphing trajectories, or electronic properties. These challenges fall under the ''inverse design'' problem, as opposed to the traditional design process that follows a ''forward'' process, where researchers start with a set of materials and designs, and then explore their properties and potential applications. Inverse design leverages computational tools and algorithms, including machine learning, evolutionary algorithm (EA), computer vision algorithm, *etc.*[74] A general inverse design involves training of the machine learning model for the forward properties' prediction, followed by the EA coupled with ML to solve the inverse problem of finding the optimal design. To date, Sun *et al.* reported the use of machine learning-EA to enable the inverse design of a 4D-printed active beam that can morph into the predicted shape upon swelling.[75] Mao *et al.* demonstrated the design of complex architectural materials with desired mechanical properties using Generative Adversarial Networks.[76] Bai *et al.* showed a linearized model-driven inverse design approach for developing a self-evolving metasurface.[77] Despite such advancements, each method continues to face challenges that need to be overcome to improve prediction accuracy and computational efficiency. For instance, current machine learning approaches for inverse design problems rely on simulated rather than experimental data, potentially resulting in higher prediction errors and providing only preliminary estimations. Meanwhile, linearized model-driven methods might not account for errors stemming from non-linearity and can become prohibitively complex computationally when attempting to incorporate non-linearity into the material system. This situation calls for further algorithmic developments to reduce computational complexity. Additionally, we contend that creating an extensive dataset from valid experimental findings would significantly promote the use of ML methods in the discovery of new materials and their properties. Recently, we developed a data-driven pipeline to extract structure–property relationships from SEM images.[78] We created a database that contains mechanical properties of interest and their corresponding SEM images using automated web-scraping and natural language processing techniques. This database was then utilized to train Convolutional Neural Networks (CNNs) to recognize and understand the mechanical properties conveyed by microstructural images. This approach could potentially open a new avenue for compiling extensive datasets from public repositories.

Integration of multi-materials with diverse functions into a highly functional device

Living organisms in nature often exhibit sophisticated functions facilitated by the seamless integration of soft active components with other structures that possess vastly different mechanical and chemical properties.[79] A simple example would be the human skin and its associated structures. The skin, a soft and flexible organ, is intricately connected with harder structures such as nails and hair. This system also involves complex, dynamic chemistries like the secretion of oils and sweat, as well as sophisticated feedback mechanisms that regulate temperature and protect against environmental damage.[80] Across multiple length scales, from the microscopic arrangement of cells and proteins to the macroscopic level of the entire organ, this integration endows the human body with properties and functions – such as protection, sensation, and thermoregulation – that are complex and still being explored in the context of replicating similar functionalities in synthetic systems. Such capabilities are particularly intriguing for

bioelectronic applications,[81–83] where integrating multifunctional features like signal transduction, sensitivity, flexibility, stability, and durability into a single device is highly desirable. However, most of the synthetic active materials rely on the material itself for computation, especially seen in soft actuators and robotics, which inherently limits the complexity of tasks they can perform. The challenge in employing active materials lies in their integration with functional devices for computational purposes. While extrusion-based 3D printing has advanced the assembly of varied materials, it remains confined to the production of soft materials. Integrating rigid computing elements like microchips into these systems requires additional fabrication steps and often leads to cumbersome systems interconnected by wires. More importantly, orders of magnitude mismatch of the mechanical properties between soft active materials and rigid computing components often cause delamination, leading to potential loss of functionality across the entire device. The development of completely soft computing components stands as a potential resolution to this issue.[84] However, there remains a significant journey ahead before soft electronic devices can match the performance of their rigid counterparts.

Development of adaptive and high-resolution extrusion-based 3D printing technology

Extrusion-based 3D printing is a powerful yet facile technique that allows for embedding the responsive characteristics of active materials into the structural design with precision and control. Research on multi-material 3D printing further expands the capabilities of extrusion-based 3D printing by allowing the integration of materials with diverse properties,[85] thereby enabling new functionalities. However, until now, this extrusion-based technique has mainly been applied to deposit soft materials in layers on flat surfaces. Nonetheless, numerous developing applications could gain significantly from the capacity to print materials with diverse compositions conformably on substrates of various shapes and contours. Work demonstrated by Uzel *et al.* points toward the future development of extrusion-based 3D printing towards multi-material, multi-nozzle, adaptive printing to conformally pattern soft materials onto arbitrary substrates.[86] Furthermore, achieving high resolution ($\sim$10 μm) extrusion-based 3D printing is favorable in many applications that require fine features of the printed structures,[87] such as wearable electronics. In general, the printing resolution of extrusion-based 3D printing depends on the rheological properties of the ink, printing parameters (*i.e.*, printing speed, pressure, *etc.*), and nozzle size. For example, efforts have been made to improve the resolution of extrusion-based 3D printing by reducing the nozzle size while tuning the molecular weight of the printed polymer, where researchers find out that a higher molecular weight results in better detail resolution.[88] However, there is a trade-off effect—if the molecular weight is too high (*i.e.*, M_w = 100 kDa) while the printing nozzle is small (*i.e.*, inner diameter = 3 μm), it will increase the clogging risk during printing. Therefore, the printing resolution is limited by the nozzle size if other parameters are fixed. Additionally, the availability of ultra-fine nozzles—those with diameters in a few micrometer range—is limited, and these nozzles tend to be costly. Yuk *et al.* tackled the restriction posted by the printing nozzle by stretching the extruded ink using a printing speed matching the extrusion velocity, such that the extruded filament exhibits a finer resolution than the nozzle diameter (for example, up to 1.9 and 5.4 times for the silicone elastomer and the hydrogel inks, respectively).[89] Nevertheless, this strategy can only be applied to inks that possess a storage modulus sufficiently robust to sustain the stretching effect. Future research is directed toward creating novel ink formulations with enhanced viscoelastic properties, alongside technological advancements in extrusion-based 3D printing. These developments may be realized through the integration of artificial intelligence to fine-tune the printing process.

Data availability statement

No primary research results, software or code have been included and no new data were generated or analysed as part of this review.

Conflicts of interest

The authors declare no conflicts of interest.

Acknowledgements

This work was supported by the National Science Foundation through the University of California San Diego Materials Research Science and Engineering Center (UCSD MRSEC), grant number DMR-2011924.

Notes and references

1 Y. Kotsuchibashi, *Polym. J.*, 2020, **52**, 681–689.
2 M. Li, J. Mei, J. Friend and J. Bae, *Small*, 2022, **18**, 2204288.
3 J. Nie, X. Chen and Z. L. Wang, *Adv. Funct. Mater.*, 2019, **29**, 1806351.
4 Y. Kim and X. Zhao, *Chem. Rev.*, 2022, **122**, 5317–5364.
5 X. Li, M. Li, L. Tang, D. Shi, E. Lam and J. Bae, *Mater. Chem. Front.*, 2023, **7**, 5989–6034.
6 Z. Li and Y. Yin, *Adv. Mater.*, 2019, **31**, 1807061.
7 E. Howard, M. Li, M. Kozma, J. Zhao and J. Bae, *Nanoscale*, 2022, **14**, 17887–17894.
8 A. Grinthal and J. Aizenberg, *Chem. Soc. Rev.*, 2013, **42**, 7072–7085.
9 P. Theato, B. S. Sumerlin, R. K. O'Reilly and I. I. I. Thomas, H. Epps, *Chem. Soc. Rev.*, 2013, **42**, 7055–7056.
10 C. W. Reynolds, in Proceedings of the 14th annual conference on Computer graphics and interactive techniques, Association for Computing Machinery, New York, NY, USA, 1987, pp. 25–34.
11 T. Vicsek, A. Czirók, E. Ben-Jacob, I. Cohen and O. Shochet, *Phys. Rev. Lett.*, 1995, **75**, 1226–1229.
12 P. Fratzl, M. Friedman, K. Krauthausen and W. Schäffner, *Active Materials*, Berlin, Boston, De Gruyter, 2022, DOI: **10.1515/9783110562064**.
13 M. Li and J. Bae, *Polym. Chem.*, 2020, **11**, 2332–2338.
14 Y. Luo, L. Zhao, G. Luo, L. Dong, Y. Xia, M. Li, Z. Li, K. Wang, R. Maeda and Z. Jiang, *Microsyst. Nanoeng.*, 2023, **9**, 1–13.
15 J.-H. Na, A. A. Evans, J. Bae, M. C. Chiappelli, C. D. Santangelo, R. J. Lang, T. C. Hull and R. C. Hayward, *Adv. Mater.*, 2015, **27**, 79–85.

16 S. C. Altıparmak and S. I. C. Daminabo, *Addit. Manuf. Front.*, 2024, **3**, 200106.
17 Z. Ji, C. Yan, B. Yu, X. Wang and F. Zhou, *Adv. Mater. Interfaces*, 2017, **4**, 1700629.
18 M. Zarek, M. Layani, I. Cooperstein, E. Sachyani, D. Cohn and S. Magdassi, *Adv. Mater.*, 2016, **28**, 4449–4454.
19 F. D. C. Siacor, Q. Chen, J. Y. Zhao, L. Han, A. D. Valino, E. B. Taboada, E. B. Caldona and R. C. Advincula, *Addit. Manuf.*, 2021, **45**, 102043.
20 Z. U. Arif, M. Y. Khalid, A. Tariq, M. Hossain and R. Umer, *Giant*, 2024, **17**, 100209.
21 Y. Yang, Y. Chen, Y. Wei and Y. Li, *Int. J. Adv. Des. Manuf. Technol.*, 2016, **84**, 2079–2095.
22 Z. Guan, L. Wang and J. Bae, *Mater. Horiz.*, 2022, **9**, 1825–1849.
23 D. B. Kolesky, R. L. Truby, A. S. Gladman, T. A. Busbee, K. A. Homan and J. A. Lewis, *Adv. Mater.*, 2014, **26**, 2966.
24 Q. Chen, J. Zhao, J. Ren, L. Rong, P. Cao and R. C. Advincula, *Adv. Funct. Mater.*, 2019, **29**, 1900469.
25 R. Woo, G. Chen, J. Zhao and J. Bae, *ACS Appl. Polym. Mater.*, 2021, **3**, 3496–3503.
26 A. S. Gladman, E. A. Matsumoto, R. G. Nuzzo, L. Mahadevan and J. A. Lewis, *Nat. Mater.*, 2016, **15**, 413–418.
27 J. Zhao and J. Bae, *Adv. Funct. Mater.*, 2022, **32**, 2200157.
28 M. A. Skylar-Scott, J. Y. Huang, A. Lu, A. H. M. Ng, T. Duenki, S. Liu, L. L. Nam, S. Damaraju, G. M. Church and J. A. Lewis, *Nat. Biomed. Eng.*, 2022, **6**, 449–462.
29 J. Zhao, S. Song, X. Mu, S. M. Jeong and J. Bae, *Nano Energy*, 2022, **103**, 107825.
30 T. J. Wallin, J. Pikul and R. F. Shepherd, *Nat. Rev. Mater.*, 2018, **3**, 84–100.
31 A. Kalkal, S. Kumar, P. Kumar, R. Pradhan, M. Willander, G. Packirisamy, S. Kumar and B. D. Malhotra, *Addit. Manuf.*, 2021, **46**, 102088.
32 X. Liu, H. Yuk, S. Lin, G. A. Parada, T.-C. Tang, E. Tham, C. de la Fuente-Nunez, T. K. Lu and X. Zhao, *Adv. Mater.*, 2018, **30**, 1704821.
33 W. Yim, J. Zhou, L. Sasi, J. Zhao, J. Yeung, Y. Cheng, Z. Jin, W. Johnson, M. Xu, J. Palma-Chavez, L. Fu, B. Qi, M. Retout, N. J. Shah, J. Bae and J. V. Jokerst, *Adv. Mater.*, 2023, **35**, 2206385.
34 S. Kyle, Z. M. Jessop, A. Al-Sabah and I. S. Whitaker, *Adv. Healthcare Mater.*, 2017, **6**, 1700264.
35 M. a S. R. Saadi, A. Maguire, N. T. Pottackal, M. S. H. Thakur, M. Md Ikram, A. J. Hart, P. M. Ajayan and M. M. Rahman, *Adv. Mater.*, 2022, **34**, 2108855.
36 S. Poppinga, C. Weisskopf, A. S. Westermeier, T. Masselter and T. Speck, *AoB Plants*, 2016, **8**, plv140.
37 L. Ren, B. Li, K. Wang, X. Zhou, Z. Song, L. Ren and Q. Liu, *Front. Mater.*, 2021, **8**, 651521.
38 H. Yang, W. R. Leow, T. Wang, J. Wang, J. Yu, K. He, D. Qi, C. Wan and X. Chen, *Adv. Mater.*, 2017, **29**, 1701627.
39 Y. Kim, H. Yuk, R. Zhao, S. A. Chester and X. Zhao, *Nature*, 2018, **558**, 274–279.
40 D. Correa, S. Poppinga, M. D. Mylo, A. S. Westermeier, B. Bruchmann, A. Menges and T. Speck, *Philos. Trans. R. Soc., A*, 2020, **378**, 20190445.
41 Y. Jiang, L. M. Korpas and J. R. Raney, *Nat. Commun.*, 2019, **10**, 128.
42 G. Wang, Y. Do, T. Cheng, H. Yang, Y. Tao, J. Gu, B. An and L. Yao, in Extended Abstracts of the 2018 CHI Conference on Human Factors in Computing Systems, Association for Computing Machinery, New York, NY, USA, 2018, pp. 1–4.
43 C. Dai, L. Li, D. Wratkowski and J. H. Cho, *Nano Lett.*, 2020, **20**, 4975–4984.
44 Y. Mao, K. Yu, M. S. Isakov, J. Wu, M. L. Dunn and H. Jerry Qi, *Sci. Rep.*, 2015, **5**, 13616.
45 C. Liu, J. Schauff, D. Joung and J.-H. Cho, *Adv. Mater. Technol.*, 2017, **2**, 1700035.
46 B. P. Chandra, in *Luminescence of Solids*, ed. D. R. Vij, Springer, US, Boston, MA, 1998, pp. 361–389.
47 F. Bacon, *Advancement of Learning*, P.F. Collier and Son, 1901.
48 C. Wang, D. Peng and C. Pan, *Sci. Bull.*, 2020, **65**, 1147–1149.
49 S. Yao, P. Swetha and Y. Zhu, *Adv. Healthcare Mater.*, 2018, **7**, 1700889.
50 X. Wang, H. Zhang, R. Yu, L. Dong, D. Peng, A. Zhang, Y. Zhang, H. Liu, C. Pan and Z. L. Wang, *Adv. Mater.*, 2015, **27**, 2324–2331.
51 C.-N. Xu, T. Watanabe, M. Akiyama and X.-G. Zheng, *Appl. Phys. Lett.*, 1999, **74**, 2414–2416.
52 D. Peng, B. Chen and F. Wang, *ChemPlusChem*, 2015, **80**, 1209–1215.
53 X. Qian, Z. Cai, M. Su, F. Li, W. Fang, Y. Li, X. Zhou, Q. Li, X. Feng, W. Li, X. Hu, X. Wang, C. Pan and Y. Song, *Adv. Mater.*, 2018, **30**, 1800291.
54 D. K. Patel, B.-E. Cohen, L. Etgar and S. Magdassi, *Mater. Horiz.*, 2018, **5**, 708–714.
55 E. Koos and N. Willenbacher, *Science*, 2011, **331**, 897–900.
56 S. Roh, D. P. Parekh, B. Bharti, S. D. Stoyanov and O. D. Velev, *Adv. Mater.*, 2017, **29**, 1701554.
57 X. Li, J. Liu, D. Li, S. Huang, K. Huang and X. Zhang, *Adv. Sci.*, 2021, **8**, 2101295.
58 Y. Dong, J. Wang, X. Guo, S. Yang, M. O. Ozen, P. Chen, X. Liu, W. Du, F. Xiao, U. Demirci and B.-F. Liu, *Nat. Commun.*, 2019, **10**, 4087.
59 A. Rodrigo-Navarro, S. Sankaran, M. J. Dalby, A. del Campo and M. Salmeron-Sanchez, *Nat. Rev. Mater.*, 2021, **6**, 1175–1190.
60 B. An, Y. Wang, Y. Huang, X. Wang, Y. Liu, D. Xun, G. M. Church, Z. Dai, X. Yi, T.-C. Tang and C. Zhong, *Chem. Rev.*, 2023, **123**, 2349–2419.
61 A. M. Duraj-Thatte, A. Manjula-Basavanna, J. Rutledge, J. Xia, S. Hassan, A. Sourlis, A. G. Rubio, A. Lesha, M. Zenkl, A. Kan, D. A. Weitz, Y. S. Zhang and N. S. Joshi, *Nat. Commun.*, 2021, **12**, 6600.
62 D. Datta, E. L. Weiss, D. Wangpraseurt, E. Hild, S. Chen, J. W. Golden, S. S. Golden and J. K. Pokorski, *Nat. Commun.*, 2023, **14**, 4742.
63 E. Stavrinidou, R. Gabrielsson, E. Gomez, X. Crispin, O. Nilsson, D. T. Simon and M. Berggren, *Sci. Adv.*, 2015, **1**, e1501136.
64 H. Sareen and P. Maes, in Conference on Human Factors in Computing Systems - Proceedings, Association for Computing Machinery, 2019.
65 H. Sareen, J. Zheng and P. Maes, in Extended Abstracts of the 2019 CHI Conference on Human Factors in Computing Systems, Association for Computing Machinery, New York, NY, USA, 2019, pp. 1–2.
66 M. H. Wong, J. P. Giraldo, S.-Y. Kwak, V. B. Koman, R. Sinclair, T. T. S. Lew, G. Bisker, P. Liu and M. S. Strano, *Nat. Mater.*, 2017, **16**, 264–272.
67 S.-Y. Kwak, J. P. Giraldo, M. H. Wong, V. B. Koman, T. T. S. Lew, J. Ell, M. C. Weidman, R. M. Sinclair, M. P. Landry, W. A. Tisdale and M. S. Strano, *Nano Lett.*, 2017, **17**, 7951–7961.
68 W. Li, N. Matsuhisa, Z. Liu, M. Wang, Y. Luo, P. Cai, G. Chen, F. Zhang, C. Li, Z. Liu, Z. Lv, W. Zhang and X. Chen, *Nat. Electron.*, 2021, **4**, 134–142.
69 J. Zhao, Y. Ma, N. F. Steinmetz and J. Bae, *ACS Macro Lett.*, 2022, **11**, 961–966.
70 T. T. S. Lew, V. B. Koman, P. Gordiichuk, M. Park and M. S. Strano, *Adv. Mater. Technol.*, 2020, **5**, 1900657.
71 M. Abdul Aziz, F. Brini, H. Rouached and K. Masmoudi, *Front. Plant Sci.*, 2022, **13**, 1027828.
72 H. Ahmad, S. Sehgal, A. Mishra and R. Gupta, *Pharmacogn. Rev.*, 2012, **6**, 115–124.
73 Y. Forterre, J. M. Skotheim, J. Dumais and L. Mahadevan, *Nature*, 2005, **433**, 421–425.
74 A. Jain, J. A. Bollinger and T. M. Truskett, *AIChE J.*, 2014, **60**, 2732–2740.
75 X. Sun, L. Yue, L. Yu, H. Shao, X. Peng, K. Zhou, F. Demoly, R. Zhao and H. J. Qi, *Adv. Funct. Mater.*, 2022, **32**, 2109805.
76 Y. Mao, Q. He and X. Zhao, *Sci. Adv.*, 2020, **6**, eaaz4169.
77 Y. Bai, H. Wang, Y. Xue, Y. Pan, J.-T. Kim, X. Ni, T.-L. Liu, Y. Yang, M. Han, Y. Huang, J. A. Rogers and X. Ni, *Nature*, 2022, **609**, 701–708.
78 B. Ho, J. Zhao, J. Liu, L. Tang, Z. Guan, X. Li, M. Li, E. Howard, R. Wheeler and J. Bae, *ACS Mater. Lett.*, 2023, **5**, 3117–3125.
79 J. R. Banavar, T. J. Cooke, A. Rinaldo and A. Maritan, *Proc. Natl. Acad. Sci. U. S. A.*, 2014, **111**, 3332–3337.
80 A. K. Dąbrowska, F. Spano, S. Derler, C. Adlhart, N. D. Spencer and R. M. Rossi, *Sking Res. Technol.*, 2018, **24**, 165–174.
81 D. M. Cox-Pridmore, F. A. Castro, S. R. P. Silva, P. Camelliti and Y. Zhao, *Small*, 2022, **18**, 2105281.
82 G. D. Goh, J. M. Lee, G. L. Goh, X. Huang, S. Lee and W. Y. Yeong, *Tissue Eng., Part A*, 2023, **29**, 20–46.
83 J. W. Phillips, A. Prominski and B. Tian, *View*, 2022, **3**, 20200157.
84 Y. Luo, M. R. Abidian, J.-H. Ahn, D. Akinwande, A. M. Andrews, M. Antonietti, Z. Bao, M. Berggren, C. A. Berkey, C. J. Bettinger, J. Chen, P. Chen, W. Cheng, X. Cheng, S.-J. Choi, A. Chortos,

C. Dagdeviren, R. H. Dauskardt, C. Di, M. D. Dickey, X. Duan, A. Facchetti, Z. Fan, Y. Fang, J. Feng, X. Feng, H. Gao, W. Gao, X. Gong, C. F. Guo, X. Guo, M. C. Hartel, Z. He, J. S. Ho, Y. Hu, Q. Huang, Y. Huang, F. Huo, M. M. Hussain, A. Javey, U. Jeong, C. Jiang, X. Jiang, J. Kang, D. Karnaushenko, A. Khademhosseini, D.-H. Kim, I.-D. Kim, D. Kireev, L. Kong, C. Lee, N.-E. Lee, P. S. Lee, T.-W. Lee, F. Li, J. Li, C. Liang, C. T. Lim, Y. Lin, D. J. Lipomi, J. Liu, K. Liu, N. Liu, R. Liu, Y. Liu, Y. Liu, Z. Liu, Z. Liu, X. J. Loh, N. Lu, Z. Lv, S. Magdassi, G. G. Malliaras, N. Matsuhisa, A. Nathan, S. Niu, J. Pan, C. Pang, Q. Pei, H. Peng, D. Qi, H. Ren, J. A. Rogers, A. Rowe, O. G. Schmidt, T. Sekitani, D.-G. Seo, G. Shen, X. Sheng, Q. Shi, T. Someya, Y. Song, E. Stavrinidou, M. Su, X. Sun, K. Takei, X.-M. Tao, B. C. K. Tee, A. V.-Y. Thean, T. Q. Trung, C. Wan, H. Wang, J. Wang, M. Wang, S. Wang, T. Wang, Z. L. Wang, P. S. Weiss, H. Wen, S. Xu, T. Xu, H. Yan, X. Yan, H. Yang, L. Yang, S. Yang, L. Yin, C. Yu, G. Yu, J. Yu, S.-H. Yu, X. Yu, E. Zamburg, H. Zhang, X. Zhang, X. Zhang, X. Zhang, Y. Zhang, Y. Zhang, S. Zhao, X. Zhao, Y. Zheng, Y.-Q. Zheng, Z. Zheng, T. Zhou, B. Zhu, M. Zhu, R. Zhu, Y. Zhu, Y. Zhu, G. Zou and X. Chen, *ACS Nano*, 2023, **17**, 5211–5295.

85 A. Nazir, O. Gokcekaya, K. Md Masum Billah, O. Ertugrul, J. Jiang, J. Sun and S. Hussain, *Mater. Des.*, 2023, **226**, 111661.

86 S. G. M. Uzel, R. D. Weeks, M. Eriksson, D. Kokkinis and J. A. Lewis, *Adv. Mater. Technol.*, 2022, **7**, 2101710.

87 Y.-G. Park, I. Yun, W. G. Chung, W. Park, D. H. Lee and J.-U. Park, *Adv. Sci.*, 2022, **9**, 2104623.

88 F. Rezaei, D. O. Carlsson, J. Hedin Dahlstrom, J. Lindh and S. Johansson, *Sci. Rep.*, 2023, **13**, 22044.

89 H. Yuk and X. Zhao, *Adv. Mater.*, 2018, **30**, 1704028.